Rapid Report

Effects of membrane potential and tension on prestin, the outer hair cell lateral membrane motor protein

Joseph Santos-Sacchi, Weixing Shen*, Jing Zheng* and Peter Dallos*

Sections of Otolaryngology and Neurobiology, Yale University School of Medicine, New Haven, CT 06510 and **Neurobiology and Physiology, Northwestern University, 2299 N. Campus Drive, Evanston, IL 60208, USA*

(Received 14 December 2000; accepted after revision 25 January 2001)

1. Under whole-cell voltage clamp, the effects of initial voltage conditions and membrane tension on gating charge and voltage-dependent capacitance were studied in human embryonic kidney cells (TSA201 cell line) transiently transfected with the gene encoding the gerbil protein prestin. Conformational changes in this membrane-bound protein probably provide the molecular basis of the outer hair cell (OHC) voltage-driven mechanical activity, which spans the audio spectrum.

2. Boltzmann characteristics of the charge movement in transfected cells were similar to those reported for OHCs ($Q_{max} = 0.99 \pm 0.16$ pC, $z = 0.88 \pm 0.02$; $n = 5$, means $\pm$ S.E.M.). Unlike that of the adult OHC, the voltage at peak capacitance (V_{pkcm}) was very negative (-74.7 ± 3.8 mV). Linear capacitance in transfected cells was 43.7 ± 13.8 pF and membrane resistance was 458 ± 123 MΩ.

3. Voltage steps from the holding potential preceding the measurement of capacitance–voltage functions caused a time- and voltage-dependent shift in V_{pkcm}. For a prepulse to −150 mV, from a holding potential of 0 mV, V_{pkcm} shifted 6.4 mV, and was fitted by a single exponential time constant of 45 ms. A higher resolution analysis of this time course was made by measuring the change in capacitance during a fixed voltage step and indicated a double exponential shift ($\tau_0 = 51.6$ ms, $\tau_1 = 8.5$ s) similar to that of the native gerbil OHC.

4. Membrane tension, delivered by increasing pipette pressure, caused a positive shift in V_{pkcm}. A maximal shift of 7.5 mV was obtained with 2 kPa of pressure. The effect was reversible.

5. Our results show that the sensitivity of prestin to initial voltage and membrane tension, though present, is less than that observed in adult OHCs. It remains possible that some other interacting molecular species within the lateral plasma membrane of the native OHC amplifies the effect of tension and prior voltage on prestin's activity.

In mammals, two classes of hair cell evolved to meet the requirements of high frequency acoustic reception. The inner hair cell, which is innervated by the majority of eighth-nerve afferents (Spoendlin, 1986), is the primary sensory receptor. The outer hair cell (OHC), while capable of generating acoustically evoked receptor potentials (Dallos *et al.* 1982), additionally functions as a mechanical effector that is thought to provide feedback to the basilar membrane to enhance auditory sensitivity and frequency resolving power (Brownell *et al.* 1985; Ashmore, 1987; Dallos, 1992).

The OHC is clearly unique. It alone is capable of voltage-induced mechanical responses ranging up to at least 100 kHz (Frank *et al.* 1999). The lateral membrane of this cylindrical cell houses the molecular machinery responsible for this response (Dallos *et al.* 1991; Kalinec *et al.* 1992; Huang & Santos-Sacchi, 1993). Recently the gene for a candidate motor protein, prestin, has been cloned (Zheng *et al.* 2000), and this protein is restricted to the lateral membrane of OHCs (Belyantseva *et al.* 2000). Prestin, in addition to enabling voltage-induced mechanical activity in transfected non-auditory cells, was shown to display some of the electrical characteristics of the native OHC sensor/motor, namely gating charge movement or non-linear capacitance that exhibits shallow voltage dependence (Zheng *et al.* 2000).

In this study we explored further the characteristics of prestin's voltage sensor, and found that similar to the native OHC motor, prestin's charge *vs.* voltage (Q–V) function possesses memory (Santos-Sacchi *et al.* 1998) and is

mechanically sensitive (Iwasa, 1993; Gale & Ashmore, 1994; Kakehata & Santos-Sacchi, 1995). That is, the motor molecule's behaviour is influenced by prior voltage conditions and membrane tension.

METHODS

The electrical characteristics of prestin and the native OHC sensor/motor were evaluated under the same conditions. Transient transfection of human embryonic kidney (TSA201) cells with gerbil prestin was performed as previously described (Zheng *et al.* 2000). Co-expression of green fluorescent protein provided visual identification of transfected cells. OHCs were freshly isolated from the cochleae of gerbils, which were killed by decapitation following anaesthetic overdose (100 mg kg^{-1} Nembutal, I.P.). This method follows the guidelines established by Northwestern and Yale University's Animal Care and Use Committees. Cells were whole-cell voltage clamped with an Axopatch 200B amplifier (Axon Instruments, CA, USA) at a holding potential of 0 mV. The patch pipette solution contained (mM): 140 CsCl, 2 $MgCl_2$, 10 EGTA, 10 Hepes; pH 7.2. The external solution contained (mM): 120 NaCl, 20 TEA-Cl, 2 $CoCl_2$, 2 $MgCl_2$, 10 Hepes, 5 glucose; pH 7.2. Osmolarity was adjusted to 300 mosmol l^{-1} with glucose. Current responses were filtered at 5 kHz. Corrections were made for the effects of residual series resistance, which averaged less than 10 MΩ. All data collection and most analyses were performed with a Windows-based whole-cell voltage-clamp program, jClamp (SciSoft, CT, USA), utilizing a National Instruments PCI-6052E 16-bit interface. Matlab (Natick, MA, USA) was used for some analyses. Fits were made with the Levenberg-Marquardt algorithm. Recordings from TSA201 cells that evidenced electrical coupling to adjacent cells were excluded from data analysis. Coupling was assessed with input capacitance measures (Santos-Sacchi, 1991*a*).

Whole-cell membrane capacitance was measured with two techniques, transient and AC. The former entailed the delivery of a stair-step voltage ranging from −160 to 120 mV, in 14 mV

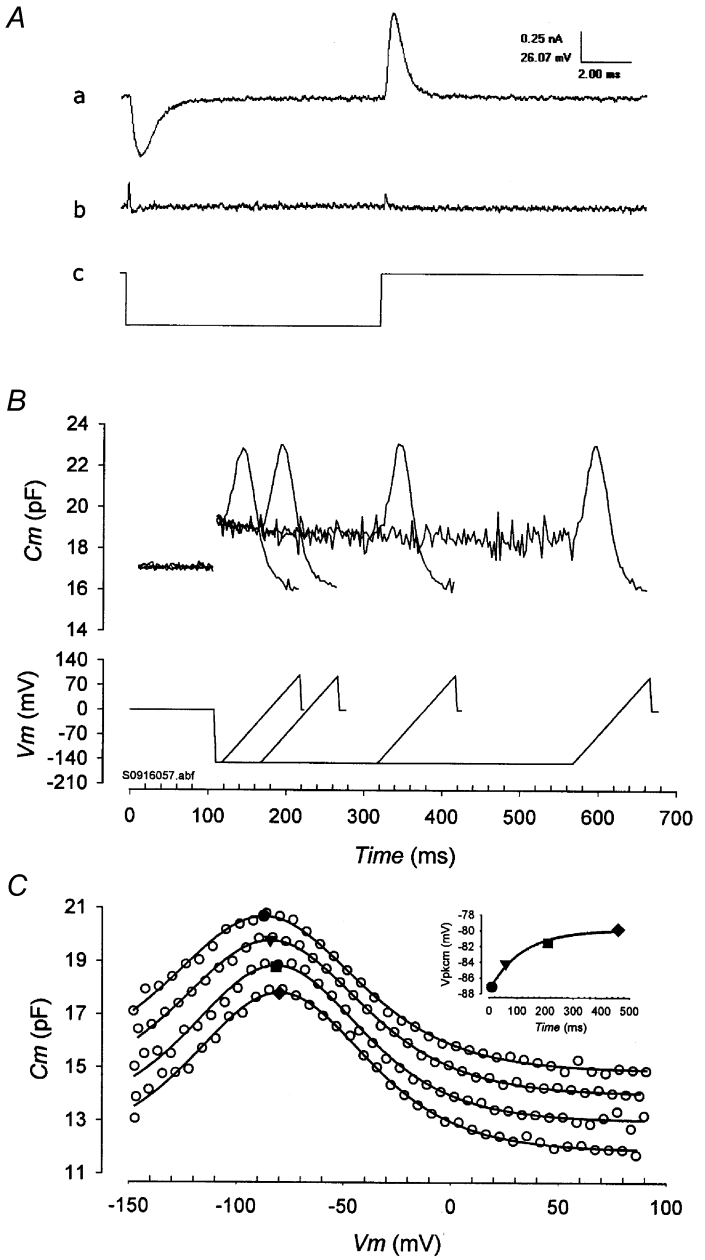

Figure 1. Prestin's charge movement is sensitive to initial voltage

A, gating current (*a*) in a prestin-transfected TSA201 cell induced by a voltage step (*c*) to −100 mV from a holding potential of 0 mV. Non-transfected cells did not produce gating currents (*b*). *P*/−4 protocol was used with a subtraction holding potential of +50 mV. *B*, whole-cell C_m determined with dual sinusoidal technique (top panel). The bottom panel shows the voltage protocol. Sinusoids have been removed for visual clarity. Data were obtained from 4 episodes; voltage was stepped to −150 mV with incrementing durations from a holding potential of 0 mV. Five-second intervals at the holding potential were allowed for recovery between episodes. *C*, capacitance data from *B* are plotted *vs.* ramp voltage. Traces are shifted downward (1 pF decrements) for visual clarity. Fits indicate a shift in V_{pkcm} denoted by ● (V_{pkcm}, Q_{max}, z and C_{lin} were, respectively: −87.15 mV, 0.89 pC, 0.66 and 14.7 pF), ▼ (−84.2 mV, 0.91 pC, 0.64 and 15.0 pF), ■ (−81.5 mV, 0.97 pC, 0.61 and 15.0 pF) and ◆ (−79.8 mV, 0.96 pC, 0.63 and 14.9 pF). The same symbols are used in the inset plot to show the time course of the shift. A single exponential fit gave $\tau = 116$ ms.

increments. Transient currents were integrated to obtain cell capacitance (C_m) measurements as previously described (Huang & Santos-Sacchi, 1993). The second technique utilized a continuous high-resolution (2.56 ms sampling) two-sine voltage stimulus protocol (10 mV peak at both 390.6 and 781.2 Hz), with subsequent fast Fourier transform (FFT)-based admittance analysis (Santos-Sacchi *et al.* 1998). These high-frequency sinusoids were superimposed on voltage ramp, step or sinusoidal stimuli. Capacitance data were fitted to the first derivative of a two-state Boltzmann function (Santos-Sacchi, 1991*b*):

$$C_m = Q_{max}\left(\frac{zeb}{kT(1+b)^2}\right) + C_{lin}, \quad (1)$$

$$b = \exp\left(\frac{-ze(V_m - V_{pkcm})}{kT}\right),$$

where Q_{max} is the maximum non-linear charge moved, V_{pkcm} is voltage at peak capacitance or half-maximal non-linear charge transfer, V_m is membrane potential, C_{lin} is linear capacitance, z is valency, e is electron charge, k is Boltzmann's constant and T is absolute temperature. Gating currents were obtained as described previously (Santos-Sacchi, 1991*b*). V_{pkcm} was tracked in real time with 2 mV resolution by monitoring the reversal of gating current polarity as fully described previously (Kakehata & Santos-Sacchi, 1995). Pipette pressure was monitored with a solid-state device (WPI, FL, USA) (Kakehata & Santos-Sacchi, 1995).

RESULTS

With ionic currents blocked, transfected TSA201 cells evidenced non-linear gating currents with characteristics similar to those obtained from native OHC lateral membrane sensor/motors (Fig. 1*Aa*). Control cells that were not transfected did not generate such currents (Fig. 1*Ab*). This result confirms the findings of Zheng *et al.* (2000). Transient analysis of the membrane capacitance arising from these gating currents provided estimates of the voltage-dependent Boltzmann characteristics of the charges. In five cells, we obtained values similar to those reported for OHCs, namely $Q_{max} = 0.99 \pm 0.16$ pC and $z = 0.88 \pm 0.02$ (means ± S.E.M.). Unlike that of the OHC, however, the voltage at peak capacitance (V_{pkcm}) was very negative (-74.7 ± 3.8 mV) at the outset of whole-cell voltage clamp. Guinea-pig OHCs had their peak non-linear capacitance at −21.5 mV (Kakehata & Santos-Sacchi, 1995). Linear capacitance in transfected cells was 43.7 ± 13.8 pF and membrane resistance was 458 ± 123 MΩ.

Voltage steps from the holding potential preceding the measurement of capacitance *vs.* voltage (C–V) functions caused a time- and voltage-dependent shift in V_{pkcm}. Figure 1*B* illustrates an example utilizing the admittance-based measurement technique. From a holding potential of 0 mV, the cell was stepped to −150 mV for 10, 60, 210 or 460 ms, after which the cell was ramped to 100 mV to obtain the C–V function. The negative prepulse caused a shift in the capacitance function in the depolarizing direction; as prepulse length increased, the magnitude of the shift increased, with a 7.3 mV shift being obtained after 460 ms. The inset in Fig. 1*C* presents the time course of the shift and shows a single exponential fit with a time constant of 116 ms. Figure 2 presents the average results obtained from such prepulse experiments; a single exponential fit to the averaged data points provided a time constant of 45 ms. In comparison, similar data obtained from native OHCs could be fitted with a time constant of about 200 ms (Santos-Sacchi *et al.* 1998). Additionally, whereas prepulse-induced, steady-state shifts of 14 mV are found in native OHCs (Santos-Sacchi *et al.* 1998), the average shift was 6.4 mV in transfected cells (Fig. 2).

We refined our estimates of the time course of the V_{pkcm} shift by measuring cell capacitance during constant voltage steps. Since a change in voltage induces a shift in the bell-shaped capacitance function along the voltage axis, at any fixed voltage the magnitude of the capacitance will change over time, and will reflect the time course of the shift in V_{pkcm} (Santos-Sacchi *et al.* 1998). Figure 3 illustrates this phenomenon for a transfected cell and a gerbil OHC. During the voltage step, the capacitance magnitudes changed with a double exponential time course. For the transfected cell τ_0 was 51.6 ms and τ_1 was 8.5 s, whereas for the OHC τ_0 was 69.2 ms and τ_1 was 2.79 s. It should be noted that the duration of the step was short relative to the second time constant values. Good fits by eye were obtained by fixing both second time constants at 1.2 s, the second time constant value obtained from OHCs when longer step durations were delivered (Santos-Sacchi *et al.* 1998).

Finally, we evaluated the effects of membrane tension on V_{pkcm}. Membrane tension, applied via pipette or osmotic pressure, is known to shift V_{pkcm} in OHCs (Iwasa, 1993; Gale & Ashmore, 1994; Kakehata & Santos-Sacchi, 1995). Figure 4 shows that changes in pipette pressure can reversibly shift V_{pkcm} in transfected cells. For example, a pipette pressure of 2 kPa resulted in a shift of about 7.5 mV. With pressures larger than 2 kPa cells were blown off the pipette or seals were lost. Changes in the

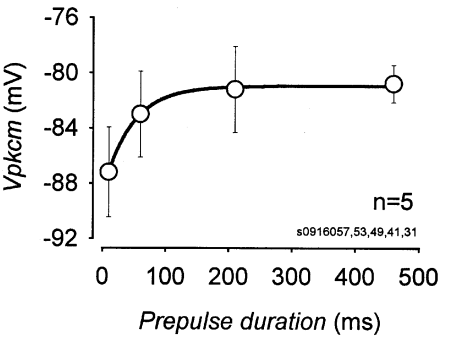

Figure 2. Average V_{pkcm} *vs.* prepulse duration

Data were obtained from experimental protocols as in Fig. 1. Plotted are the means ± S.E.M. for five transfected cells. The single exponential fit gave $\tau = 45$ ms.

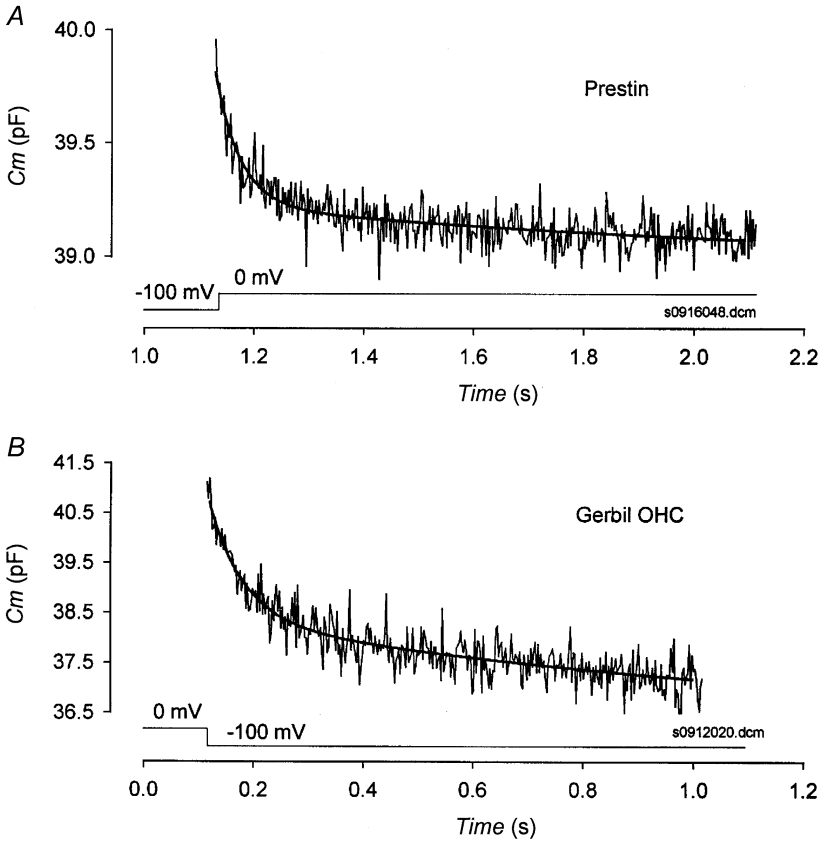

Figure 3. Time course of capacitance change following voltage step

A, transfected cell capacitance decreased with $\tau_0 = 51.6$ ms and $\tau_1 = 8.5$ s indicative of the time-dependent shift in V_{pkcm}. *B*, OHC capacitance decreased with $\tau_0 = 69.2$ ms and $\tau_1 = 2.79$ s. These results are predicted by a visco-elastic model of motor interactions (Santos-Sacchi *et al.* 1998).

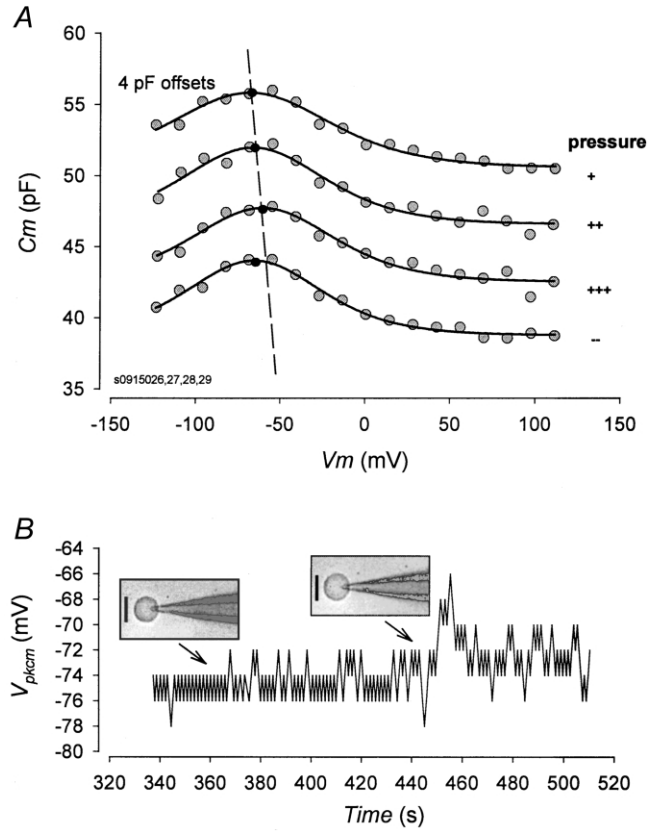

Figure 4. Effects of membrane tension on V_{pkcm}

A, *C–V* functions were obtained with transient analysis under conditions where pipette pressure was modified. Capacitance functions are offset by −4 pF for visual clarity. ●, fitted V_{pkcm}. A straight line is drawn through the top three values, indicating the depolarizing shift in V_{pkcm} that accompanied pipette pressure increases. Pipette pressure was less than 0 kPa (− −), ∼0.6 kPa (+), ∼1.3 kPa (+ +) and ∼2 kPa (+ + +). When pressure was made negative, V_{pkcm} shifted back in the hyperpolarizing direction. Fits (from top trace to bottom trace) for V_{pkcm}, Q_{max}, z and C_{lin} were, respectively: −68.0 mV, 0.81 pC, 0.66 and 50.6 pF; −66.2 mV, 0.91 pC, 0.60 and 50.6 pF; −60.5 mV, 0.91 pC, 0.58 and 50.5 pF; −65.4 mV, 0.96 pC, 0.55 and 50.8 pF. *B*, V_{pkcm} was tracked during changes in pipette pressure. Photographs of patch-clamped transfected cells correspond to points (arrows) before and after a pressure increase that changed cell diameter by 8%. A slight depolarizing shift in V_{pkcm} was observed during the pressure increase.

dimensions of the cells confirmed that pipette pressure was delivered to the cells (Fig. 4*B*). The magnitude of the response was small compared to that of OHCs where shifts as large as 50 mV are found (Kakehata & Santos-Sacchi, 1995).

DISCUSSION

Non-linearity is the hallmark of the mammalian auditory system's active process whereby near-threshold responses are selectively enhanced. In fact, a variety of non-linear phenomena exist within single OHCs that identify candidate mechanisms likely to underlie the 'cochlear amplifier'. These include non-linearities intrinsic to the mechanics of the cell soma, as well as those of the stereociliary bundle. Within the soma several non-linear, voltage-dependent processes have been studied, including electromotility (Brownell *et al.* 1985; Ashmore, 1987; Santos-Sacchi & Dilger, 1988), stiffness (He & Dallos, 1999) and membrane lipid mobility (Oghalai *et al.* 2000). Recently, we showed that the very same stimulus, i.e. lateral membrane voltage, that evokes OHC somatic mechanical activity influences its form (Santos-Sacchi *et al.* 1998). We successfully modelled the effect as a visco-elastic interaction among lateral membrane motor molecules, where motor-induced membrane tension shifted the cell's *C*–*V* function. One of the consequences of this interaction is similar to that occurring within the stereociliary bundle, namely that a shift in the operating point of the transducer function over time provides for differing instantaneous and steady-state responsiveness. Consequently, in the case of the OHC soma, we observe hysteresis in the *C*–*V* or *Q*–*V* function, the magnitude of which may be frequency dependent (J. Santos-Sacchi & E. Navarrete, unpublished observation). Even at the system level, susceptibility of the motor to membrane tension underlies the generation of non-linearities resulting from mechanical interactions among OHCs within the organ of Corti (Zhao & Santos-Sacchi, 1999). Our present observation that prestin displays the same complex electrical characteristics, and attendant non-linearities, as those of the native OHC motor confirms the identity of this protein. Since prestin presents these qualities in the absence of its normal cellular environment, our work also raises questions about the molecular requirements for full functional activity.

There are several features that differentiate OHCs from other hair cells. Most notably, the OHC possesses an extensive composite lateral wall, consisting of the mechanically active lateral plasma membrane, the cortical cytoskeleton and the subsurface cisternae (Flock *et al.* 1986; Holley *et al.* 1992; Pollice & Brownell, 1993). Structural distinctions such as these probably underscore a functional requirement for unique protein constituents, and indeed, besides prestin, other proteins specific to the OHC are known to exist (Sakaguchi *et al.* 1998; Zheng *et al.* 2000). While it is possible that novel auxiliary protein subunits act in conjunction with prestin to modify its behaviour, as occurs for ionic channels (Walker & De Waard, 1998), our present results indicate that other unique proteins present in the normal OHC are not required for the generation of voltage-induced or tension-induced shifts in V_{pkcm}. We had previous indications of this autonomy, since we demonstrated that neither of the effects was abolished in OHCs by destruction of intracellular constituents with trypsin or pronase (Kakehata & Santos-Sacchi, 1995; Santos-Sacchi *et al.* 1998).

Notwithstanding the many electrical properties of the lateral membrane motor that appear intrinsic to prestin, auxiliary subunit contributions cannot be ruled out. In this regard, we found that V_{pkcm} values in transfected cells are very negative relative to those found in adult OHCs (−74.7 *vs.* −21.5 mV; Kakehata & Santos-Sacchi, 1995). Two physiological mechanisms that are capable of shifting V_{pkcm} are membrane tension (Iwasa, 1993; Gale & Ashmore, 1994; Kakehata & Santos-Sacchi, 1995) and phosphorylation (Frolenkov *et al.* 2000). While the voltage dependencies that we found may simply result from differences in resting membrane tension between transfected cells and OHCs, or from differences in the degree of phosphorylation, it is also possible that auxiliary subunits can contribute. Indeed, the voltage-dependent Ca^{2+} channel β subunit is known to shift the voltage dependence of the channel's activation (De Waard *et al.* 1994). Interestingly, during the development of rat OHCs, V_{pkcm} shifts from hyperpolarized levels to more depolarized levels as found in adult guinea-pig OHCs over the course of a few days (Oliver & Fakler, 1999). Although Oliver & Fakler (1999) argued in favour of phosphorylation over subunit interaction, the issue remains open. Finally, we note that the magnitude of the effects that we observed in the present study is not as great as that seen in native OHCs (Kakehata & Santos-Sacchi, 1995; Santos-Sacchi *et al.* 1998). Thus, while the intrinsic properties of a single protein, prestin, may form the basis of mammalian auditory system responsiveness, it remains possible that some other interacting molecular species within the lateral plasma membrane amplifies the effect of tension and prior voltage on prestin's activity. One such candidate protein is the sugar transporter GLUT-5, which localizes to the OHC lateral membrane and may influence the OHC motor (Géléoc *et al.* 1999; Belyantseva *et al.* 2000). GLUT-5 is not expressed in TSA201 cells (J. Zheng, unpublished data). Notwithstanding this scenario, it should be noted that another possibility, not yet examined, is that intrinsic constituents of the TSA201 cell's plasma membrane could influence the activity of an expressed foreign protein. Nevertheless, it is certainly clear that with the identification of prestin and other novel OHC proteins, the issue of molecular interactions within the OHC's mechanically active lateral plasma membrane can be directly assessed.

Ashmore, J. F. (1987). A fast motile response in guinea-pig outer hair cells: the cellular basis of the cochlear amplifier. *Journal of Physiology* **388**, 323–347.

Belyantseva, I., Adler, H. J., Curi, R., Frolenkov, G. I. & Kachar, B. (2000). Expression and localization of Prestin and the sugar transporter GLUT-5 during development of electromotility in cochlear outer hair cells. *Journal of Neuroscience* **20**, RC116.

Brownell, W. E., Bader, C. R., Bertrand, D. & de Ribaupierre, Y. (1985). Evoked mechanical responses of isolated cochlear outer hair cells. *Science* **227**, 194–196.

Dallos, P. (1992). The active cochlea. *Journal of Neuroscience* **12**, 4575–4585.

Dallos, P., Evans, B. N. & Hallworth, R. (1991). Nature of the motor element in electrokinetic shape changes of cochlear outer hair cells. *Nature* **350**, 155–157.

Dallos, P., Santos-Sacchi, J. & Flock, A. (1982). Intracellular recordings from cochlear outer hair cells. *Science* **218**, 582–584.

De Waard, M., Pragnell, M. & Campbell, K. P. (1994). Ca^{2+} channel regulation by a conserved beta subunit domain. *Neuron* **13**, 495–503.

Flock, A., Flock, B. & Ulfendahl, M. (1986). Mechanisms of movement in outer hair cells and a possible structural basis. *Archives of Otorhinolaryngology* **243**, 83–90.

Frank, G., Hemmert, W. & Gummer, A. W. (1999). Limiting dynamics of high-frequency electromechanical transduction of outer hair cells. *Proceedings of the National Academy of Sciences of the USA* **96**, 4420–4425.

Frolenkov, G. I., Mammano, F., Belyantseva, I. A., Coling, D. & Kachar, B. (2000). Two distinct Ca^{2+}-dependent signaling pathways regulate the motor output of cochlear outer hair cells. *Journal of Neuroscience* **20**, 5940–5948.

Gale, J. E. & Ashmore, J. F. (1994). Charge displacement induced by rapid stretch in the basolateral membrane of the guinea-pig outer hair cell. *Proceedings of the Royal Society* B **255**, 243–249.

Géléoc, G. S., Casalotti, S. O., Forge, A. & Ashmore, J. F. (1999). A sugar transporter as a candidate for the outer hair cell motor. *Nature Neuroscience* **2** , 713–719.

He, D. Z. & Dallos, P. (1999). Somatic stiffness of cochlear outer hair cells is voltage-dependent. *Proceedings of the National Academy of Sciences of the USA* **96**, 8223–8228.

Holley, M. C., Kalinec, F. & Kachar, B. (1992). Structure of the cortical cytoskeleton in mammalian outer hair cells. *Journal of Cell Science* **102**, 569–580.

Huang, G. & Santos-Sacchi, J. (1993). Mapping the distribution of the outer hair cell motility voltage sensor by electrical amputation. *Biophysical Journal* **65**, 2228–2236.

Iwasa, K. H. (1993). Effect of stress on the membrane capacitance of the auditory outer hair cell. *Biophysical Journal* **65**, 492–498.

Kakehata, S. & Santos-Sacchi, J. (1995). Membrane tension directly shifts voltage dependence of outer hair cell motility and associated gating charge. *Biophysical Journal* **68**, 2190–2197.

Kalinec, F., Holley, M. C., Iwasa, K. H., Lim, D. J. & Kachar, B. (1992). A membrane-based force generation mechanism in auditory sensory cells. *Proceedings of the National Academy of Sciences of the USA* **89**, 8671–8675.

Oghalai, J. S., Zhao, H. B., Kutz, J. W. & Brownell, W. E. (2000). Voltage- and tension-dependent lipid mobility in the outer hair cell plasma membrane. *Science* **287**, 658–661.

Oliver, D. & Fakler, B. (1999). Expression density and functional characteristics of the outer hair cell motor protein are regulated during postnatal development in rat. *Journal of Physiology* **519**, 791–800.

Pollice, P. A. & Brownell, W. E. (1993). Characterization of the outer hair cell's lateral wall membranes. *Hearing Research* **70**, 187–196.

Sakaguchi, N., Henzl, M. T., Thalmann, I., Thalmann, R. & Schulte, B. A. (1998). Oncomodulin is expressed exclusively by outer hair cells in the organ of Corti. *Journal of Histochemistry and Cytochemistry* **46**, 29–40.

Santos-Sacchi, J. (1991*a*). Isolated supporting cells from the organ of Corti: some whole cell electrical characteristics and estimates of gap junctional conductance. *Hearing Research* **52**, 89–98.

Santos-Sacchi, J. (1991*b*). Reversible inhibition of voltage-dependent outer hair cell motility and capacitance. *Journal of Neuroscience* **11**, 3096–3110.

Santos-Sacchi, J. & Dilger, J. P. (1988). Whole cell currents and mechanical responses of isolated outer hair cells. *Hearing Research* **35**, 143–150.

Santos-Sacchi, J., Kakehata, S. & Takahashi, S. (1998). Effects of membrane potential on the voltage dependence of motility-related charge in outer hair cells of the guinea-pig. *Journal of Physiology* **510**, 225–235.

Spoendlin, H. (1986). Receptoneural and innervation aspects of the inner ear anatomy with respect to cochlear mechanics. *Scandanavian Audiology* (suppl.) **25**, 27–34.

Walker, D. & De Waard, M. (1998). Subunit interaction sites in voltage-dependent Ca^{2+} channels: role in channel function. *Trends in Neurosciences* **21**, 148–154.

Zhao, H. B. & Santos-Sacchi, J. (1999). Auditory collusion and a coupled couple of outer hair cells. *Nature* **399**, 359–362.

Zheng, J., Shen, W., He, D. Z., Long, K. B., Madison, L. D. & Dallos, P. (2000). Prestin is the motor protein of cochlear outer hair cells. *Nature* **405**, 149–155.

Acknowledgements

This work was supported by NIH-NIDCD grant DC00273 to J.S.-S. and DC00708 to P.D.

Corresponding author

J. Santos-Sacchi: Surgery (Otolaryngology), BML 244, Yale University School of Medicine, 333 Cedar Street, New Haven, CT 06510, USA.

Email: joseph.santos-sacchi@yale.edu